

INVESTIGATION OF THE HYDROGEN COMBUSTION CHAMBER PERFORMACE WITHIN THE HEXAFLY-INT PROJECT

M.A. Ivankin*, A.A. Nikolaev*, V.A. Talyzin*, O.V. Voloschenko*
*** Central Aerohydrodynamics Institute n.a. prof. N.E. Zhukovsky (TsAGI)**

Keywords: *combustion chamber, hydrogen, connected-pipe facility*

Abstract

The paper presents results of experimental investigations operation of the hydrogen combustion chamber. Combustion chamber was designed, manufactured and tested within the international project HEXAFLY-INT. Tests were carried out at the connected pipe T-131 facility of TsAGI. Influence of the various fuel injection strategy on the combustion chamber efficiency in wide range of free-stream Mach numbers $M=6-7.4$ and ER coefficients was defined.

1 Introduction

In framework of the European project LAPCAT-II [1] several high-speed passenger vehicle concepts were studied on the basis of hydrogen fuelled air breathing engines. Aim of this work was to assess the technical feasibility of a high-speed vehicle for civil transportation that could fly to diametrically opposite points (e.g. from Brussels to Sydney) at cruise speeds ranging from Mach number $M_\infty=5$ to 8. The claimed performances were verified on the basis of simulations and ground-experiments. The next step is the verification by flight experiment which is one of the main goals of the international coordinated project HEXAFLY-INT.

Two concepts were proposed for study. A first concept is a glider vehicle, i.e. without any on-board propulsion. A second concept is a powered concept, i.e. with propulsion system. The first concept will evolve into in flight experiment while the second concept is studied experimentally on-ground by Russian entities

such as TsAGI and CIAM. For the experimental investigations, a powered concept Experimental Flight Test Vehicle (EFTV) with length $L=3$ m was designed (Figure 1) [2, 3].

Main purpose of experimental studies is to define the limits of stable operation of the combustion chamber in the connected-pipe test campaigns at TsAGI T-131 facility. Beside this it's also important to study the regimes at which self-ignition and flame stabilization are assured.

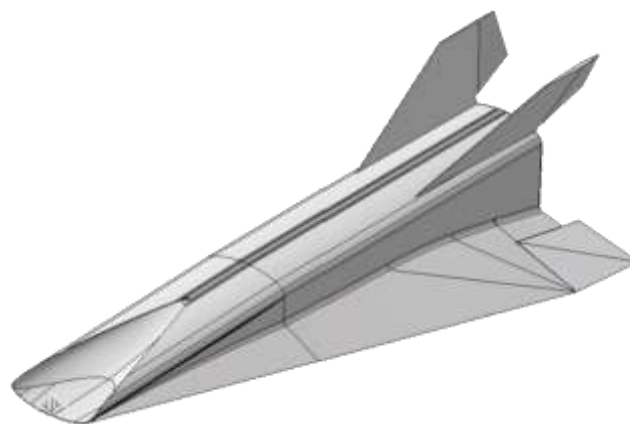


Fig. 1. Experimental Flight Test Vehicle (EFTV)

2 Model of the Elliptical Combustion Chamber

The combustion chamber for civil high-speed vehicle that is intended to be tested when been mounted on the connected-pipe facility is composed of the seven separate sections (Figure 2): an intermediate part of the direct air heater, a critical insert, a part of the supersonic nozzle, a pre-injector section with two semi-struts, a section of combustion chamber with

full-strut, a section of the 2D-nozzle and a section of the 3D-nozzle. All the sections are interconnected through the connecting flanges.

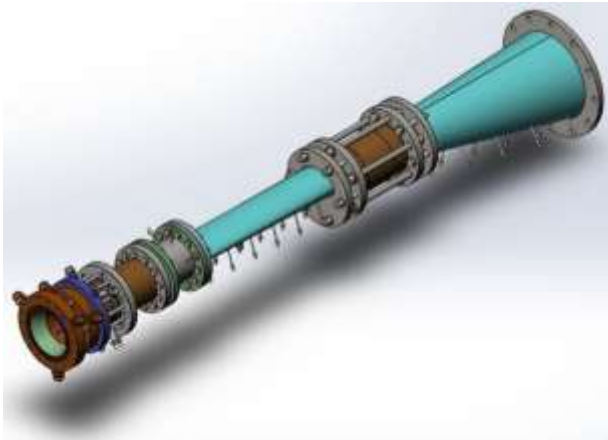


Fig. 2. Model of the elliptical combustion chamber

The combustion chamber is attached to the T-131 connected pipe facility through the cooled conic adaptor that is located at TsAGI test bench.

The semi-strut (Figure 3) has an arrow-shaped geometry with the leading edge radius of $R_1=2$ mm and the trailing edge radius of $R_2=0.3$ mm. The semi-strut is made of the heat-resistant steel. The injector exit diameter is 5 mm and the duct diameter is 4 mm. The struts are located in such a way that the fuel is supplied into the inner pipe of chamber under the given angle of 60° relative to the air stream.

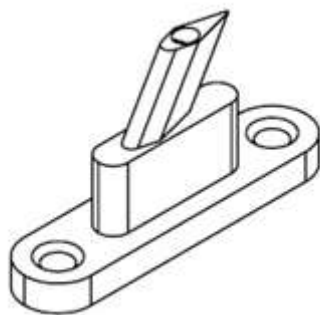


Fig. 3. Semi-strut

The full-strut (Figure 4) has an arrow-shaped geometry with the leading edge radius of $R_1=2$ mm and the trailing edge radius of $R_2=0.2$ mm. The strut is made of the heat-resistant steel. The full-strut has four holes of diameter 1.4 mm. The holes are located on two wedge surfaces (angle of 34.2°) in such a way

that the fuel supply is provided as downstream. The duct diameter is 4 mm.

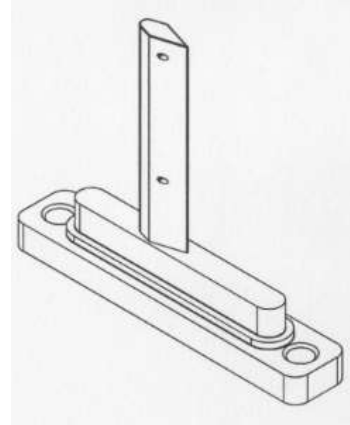


Fig. 4. Full-strut

The full-strut is installed in the section of the combustion chamber with 3° angle of taper (Figure 5). The inlet and outlet section cross-sections are ellipses with axial sizes of 48.6×133 mm and 81×133 mm.

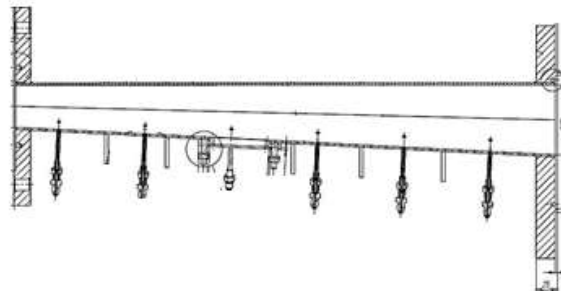


Fig. 5. Section of the combustion chamber

The 2D-nozzle has three sections (Figure 6). The section in assembly forms the combustion chamber airflow duct with annular exit cross-section of $\varnothing 133$ mm. The static pressure measuring points are located in the first and second sections (three items totally). The chamber sections are made of stainless steel.

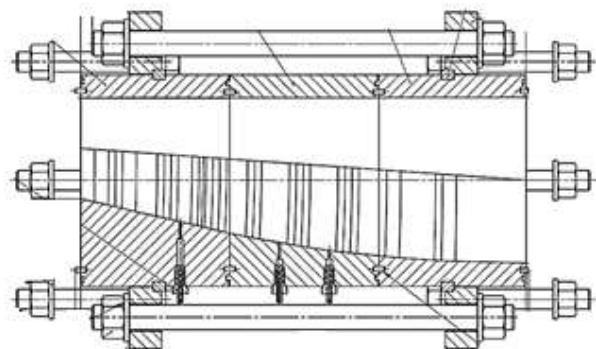


Fig. 6. Section of the 2D-nozzle

The section of the 3D-nozzle is a cone of 14° angle of taper (Figure 7). The inlet cross-section is of 133 mm diameter and the outlet one is of 301 mm. The hot wall is of 2 mm width. The material is heat-resistant steel. Three rows of static pressure gauging/measuring points (15 points totally) are located along the section duct.

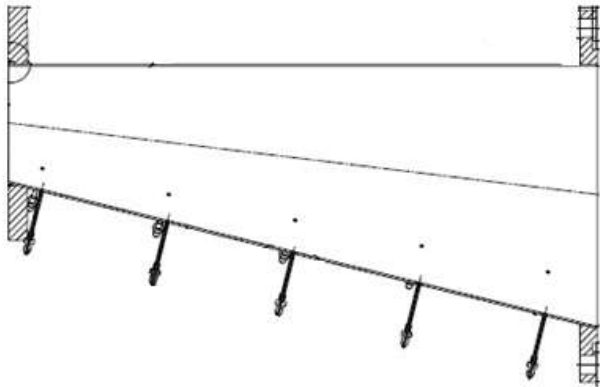


Fig. 7. Section of the 3D-nozzle

In the course of connected-pipe tests, the static pressures are measured along the installation duct in 44 points, 3 rows of measurements.

Model of the combustion chamber was manufactured by CIAM and was delivered to TsAGI for testing.

3 Facility T-131 TsAGI

The tests of the elliptical combustion chamber are carried out on the T-131 facility (Figure 8) that is intended to study:

- Operational processes in ramjet models;
- Various fuels carburation and burning processes in subsonic and supersonic flows;
- Thermal transformations of hydrocarbon fuel;
- Heat-shielding and structural materials;
- High speed air-feed jet engine models in free stream;
- Burning on the outer surfaces of flying vehicles;
- Air-feed jet engine air intakes.

The key component of the facility is a kerosene air heater of the gas-flame type. The air, the oxygen and the kerosene are supplied into the air heater combustion chamber in

amount that is needed to create a flow with the T_0 and P_0 predetermined stagnation parameters. It is to be noted that the oxygen is supplied into the air heater combustion chamber to replenish the burnt oxygen from air in such a way that the oxygen portion in products of combustion be $g_{ox}=0.232$. The last requirement is of importance for simulating the atmospheric air when testing the processes of burning. Such a manner of compensation provides also the high completeness of kerosene burning.

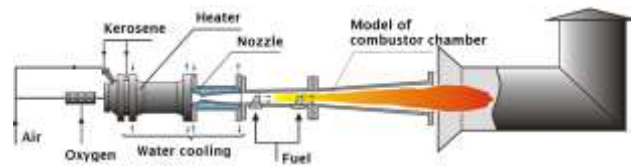


Fig. 8. Scheme of the T-131 facility

As a fuel, the air-heater uses the kerosene with the comparative weigh percentage as follows: 13.4 % of hydrogen and 86.6 % of carbon, with the stoichiometric air ratio as $L_0=14.75$, the calorific capacity of 10250 kcal/kg. The oxygen weight share in air is 0.232. In order the oxygen portion in combustion products that are produced by the air heater will correspond to the pure air, the flow rates of the kerosene and the oxygen that are supplied to the air heater must be interrelated. There are correlations of components that come in/out of the heater under the accurate keeping the oxygen portion that is equal to 0.232.

It is to be noted that there is a possibility to carry out the tests without keeping the oxygen mass portion in combustion products of air heater that corresponds to the pure air. This widens essentially the range of gas flow composition and parameters at the air heater exit.

The air preheater operates persistently under temperature range of $T_0 = 850 - 2350$ K and pressures up to 10 MPa. The operational area of the air preheater is given in the Figure 9. The upper operational area boundary conditioned by the pressure p_0 and the temperature T_0 of the air preheater gas is limited nowadays by the $p_0 = 10$ MPa pressure maximally available in the fuel system. The lower limit is estimated by the

minimally possible $p_0=0.2$ MPa pressure gradient at the fuel injectors, under which the sustainable air preheater operation is being kept. The right boundary ($T_0=2350$ K) is estimated by the maximal oxygen flow rate of 1.5 kg/s and the left one ($T_0=850$ K) – is estimated by the ranges of ignition and kerosene combustion stabilization in the air preheater.

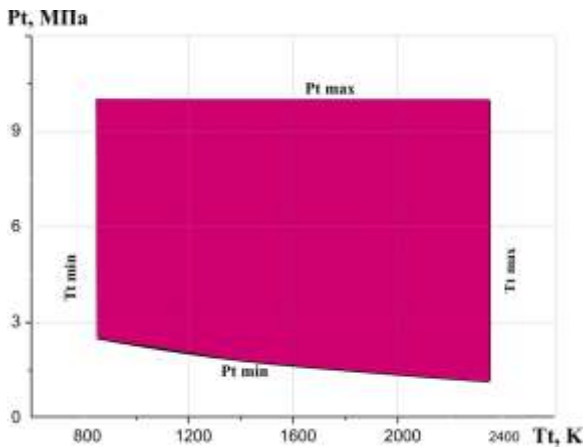


Fig. 9. Limitations of the heater's regimes

The fuel supply system of the test-bench makes it possible to carry out the experiments with various types of fuels and with providing the wide range of excess air coefficients α or excess fuel coefficients ER ($ER=1/\alpha$). Concurrently the pylon-injectors of various shapes/geometries may be used to supply fuel. Figure 10 shows struts calibration graph (correlation between mass flow through strut and pressure after reducers).

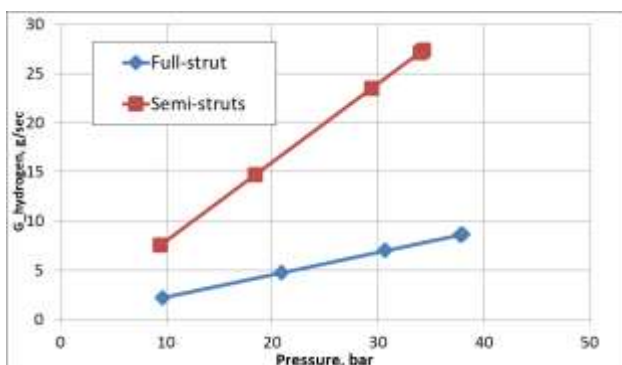


Fig. 10. Calibration of the semi-struts and the full-strut

In the Figure 11 one could see model of the elliptical combustion chamber mounted onto the facility.



Fig. 11. Model mounted onto the facility T-131 TsAGI

4 Results and Discussions

At present time investigation of the high-speed combustion chamber at the flow conditions at the duct entry corresponding to Mach numbers $M=6; 7; 7.4$ was performed. Unfortunately in tests simulated free-stream Mach number $M=7; 7.4$ full-strut has been burned, so most of the tests were conducted in case of fuel supplying only from the semi-struts in wide range of ER coefficient. Besides these tests, some tests with imitator-strut installed instead of the full-strut were done. This imitator was made from molybdenum with protective coating of the external surface. Imitator had thickness and fillet close to full-strut geometry but it hadn't duct and holes for hydrogen supply.

Main characteristics of the tests are presented in the Table 1. Results are shown in form of static pressure distribution along model's duct graphs for two main regimes: without hydrogen (cold regime) and with hydrogen (hot regime) supply. In all graphs location of the struts in shown by solid red line for semi-struts and by dash line for full-strut.

Investigation shows that at every tested conditions of the flow at the model's entry p_0 , T_0 , M and ways to inject different amount of hydrogen (in terms of the ER coefficient) self-ignition have taken place with increasing of the static pressure along the duct. Location of the maximum values of the static pressure in the model and its level have depended on conditions of the flow at the model's entry, ways and amount of supplying hydrogen (in terms of the ER coefficient).

**INVESTIGATION OF THE HYDROGEN COMBUSTION CHAMBER
PERFORMANCE WITHIN THE HEXAFLY-INT PROJECT**

No	M _∞	G _{flow} , kg/sec	G _{hyd} , g/sec	α	ER	Imitator
1	7.0	1.55	42.3 36/6	1.07	0.93	Full-strut
2	7.0	1.55	52.1 44/8	0.87	1.15	Full-strut
3	7.0	1.55	19.1	2.37	0.42	-
4	7.0	1.55	29.1	1.56	0.64	-
5	7.0	1.56	43.2	1.05	0.95	-
6	7.0	1.54	36.3	1.24	0.81	-
7	7.4	0.71	18.3	1.13	0.88	-
8	7.4	0.71	16	1.30	0.77	-
9	7.4	0.69	26.6	0.76	1.32	-
10	7.4	0.69	23.8	0.85	1.18	+
11	7.4	0.69	13.9	1.45	0.69	+
12	6.0	1.63	44.7	1.06	0.94	+
13	6.0	1.63	45.8	1.04	0.96	-
14	6.0	1.59	34	1.37	0.73	-
15	6.0	1.59	27.2	1.71	0.59	-
16	6.0	1.62	26.3	1.80	0.56	+
17	6.0	1.63	29.9	1.59	0.63	+
18	6.0	1.61	23.2	2.03	0.49	+
19	6.0	1.69	18.4 10/8	2.68	0.37	Full-strut
20	6.0	1.66	37.4 20/16	1.30	0.77	Full-strut
21	6.0	1.69	36.9 19/18	1.34	0.75	Full-strut
22	6.0	1.66	25.6 15/10	1.89	0.53	Full-strut
23	6.0	1.66	28.6 18/10	1.69	0.59	Full-strut

Table 1. Conditions of the conducted tests

Let discuss main results that were achieved in runs 1 and 2 (Figure 12) at the conditions of the flow corresponding to free-stream Mach number $M=7$ and with supplying fuel via semi-struts and full-strut. In this tests when fuel was injected static pressure war rising 2.5-3 times higher in comparison with regime without hydrogen (cold regime). That could prove fact that burning is really taking place inside the model. It could be noticed that maximum value of the static pressure in the centerline of the model locates at the distance 150-200 mm downstream the full-strut and at the right and left rows maximum locates upstream the full-strut that could be one of the reasons of the full-strut burning. Also it should be said that based

on the static pressure distribution and run recording main heat release is located in the section with full-strut and in 2D-nozzle and 3D-nozzles sections (pre-last and last sections of the model correspondingly) heat release is absent and value of the static pressure is the same at two regimes (without hydrogen and with hydrogen).

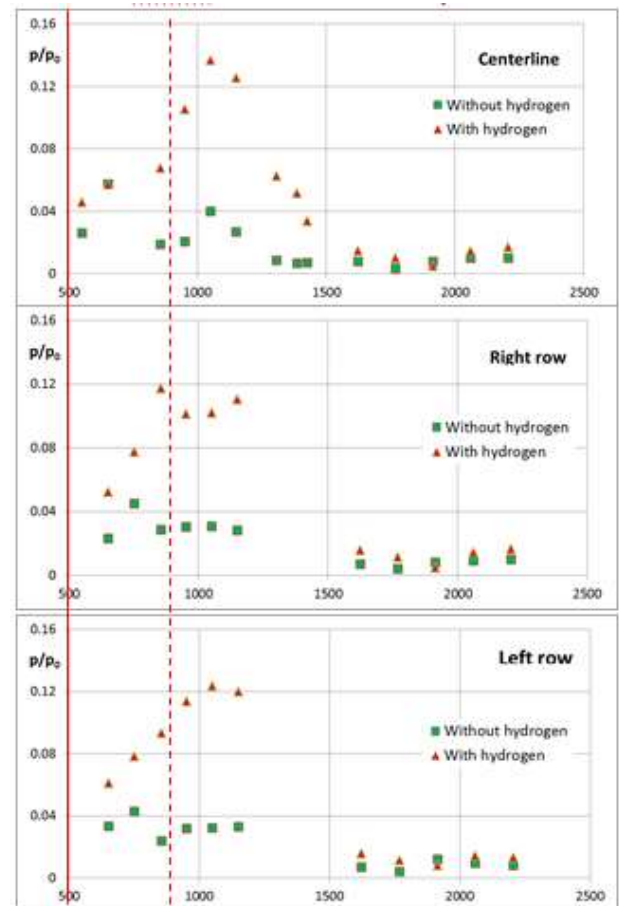


Fig. 12. Distribution of the static pressure along the duct in run 1

Let turn to data obtained in runs 3-6 at the same Mach number at the combustion chamber entry that was in runs 1-2 which corresponds to free-stream Mach number $M=7$. But at these tests fuel was injected only from the semi-struts. Tests were conducted in wide range of the ER coefficient $ER=0.42-1$. It should be noticed that raising of the static pressure (at least 1.5-2 times) was obtained only in tests in which value of the $ER>0.77$. Maximum value of the static pressure was again (like in case of hydrogen injection through semi-struts and the full-strut) located nearby the place where full-strut should

be located. At the value of the $ER < 0.77$ maximum value of the static pressure has shifted downstream to the 2D-nozzle section that could be also proved by snapshots of the runs (Figure 13).

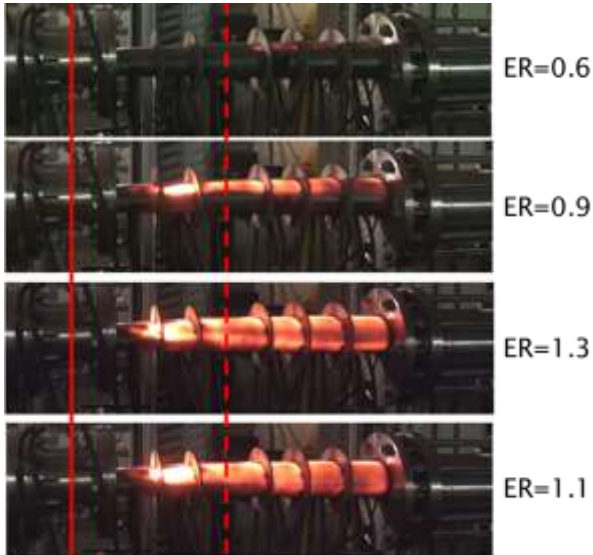


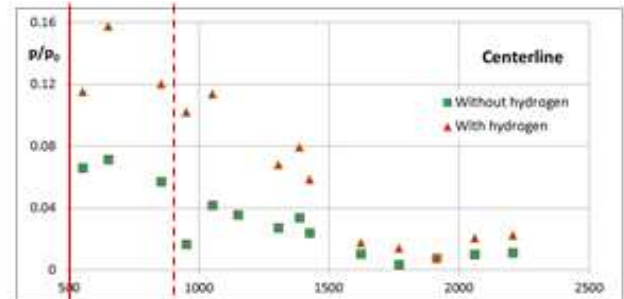
Fig. 13. Snapshots of the main regime of hydrogen burning inside the model in runs with fuel injections only from the semi-struts

Based on the result that have been discussed above some investigation of the imitator-strut influence on the working process inside combustion chamber model was carried out at Mach numbers at the model's entry corresponding to free-stream Mach numbers $M=6; 7.4$. It should be stressed that in all runs of this test campaign hydrogen was supplied only from the semi-struts.

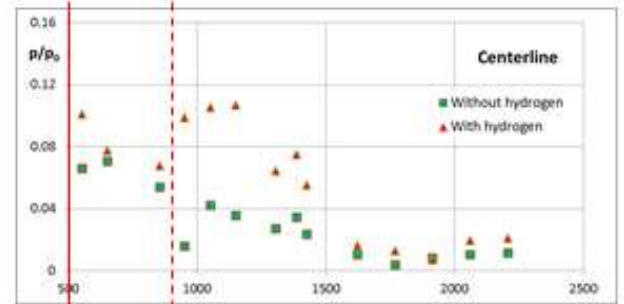
In all investigated regimes at Mach number $M=7.4$ in runs 7-11 stabilization of the burning was achieved only at the ER coefficient $ER=1.35$ (without imitator-strut) and $ER=1.2$ (with imitator-strut) with twice increasing of the static pressure. Moreover presence of the imitator-strut increasing maximum value of the static pressure in the duct and shifted its peak a little bit upstream.

If one analyses results achieved at Mach number at the entry corresponding to free-stream Mach number $M=6$ in runs 12-18, it could be concluded that burning was inside the model in all range of the ER coefficient changing $ER=0.4-1.3$ in both cases with or without imitator-strut. In runs 12-18 influence of the

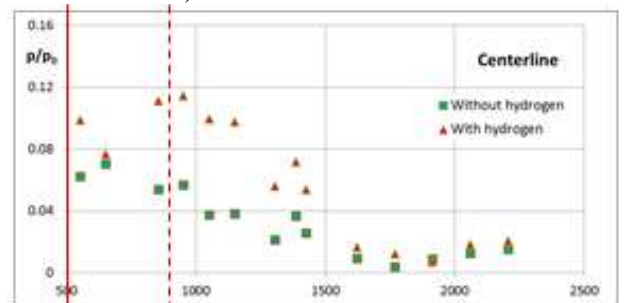
imitator-strut presence could be highlighted clearer. If one will compare results achieved in runs 12 and 13; 15 and 16 in which regimes close to each other (in terms of ER coefficient) were realized.



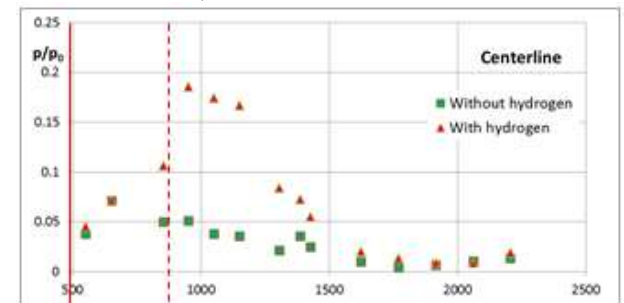
a) without imitator with increased static pressure upstream propagation (in the supersonic part of the aerodynamic nozzle) – run 13



b) without imitator – run 15



c) with imitator – run 16



d) with fuel injection from the full-strut (35% from total amount of hydrogen) – run 23

Fig. 14. Distribution of the static pressure along the centerline of the model at the entry Mach number corresponding to the free-stream Mach number $M=6$

Due to graphs (Figure 14) of the static pressure distribution it could be concluded that presence of the imitator-strut increasing maximum value of the static pressure and shifted it upstream. Moreover in run 13 in which ER coefficient was close to 1 increasing of the static pressure propagates so high upstream that could influence on the static pressure in supersonic part of the aerodynamic nozzle. Such regimes are very dangerous for propulsion because could lead to buzzing of the intake. Also it could be concluded that imitator-strut could lead to thermal choking in the place where it is installed what will increase maximum value of the static pressure and shift its peak upstream, It should be noticed that after 6 runs imitator-strut has no visual changes on the external surface.

In runs 19-23 hydrogen injection from both semi-struts and full-strut at conditions of the flow at the model's entry corresponding to free-stream Mach number $M=6$ was under investigation. In runs 19-23 self-ignition and flame stabilization without propagation to the supersonic part of the aerodynamic nozzle were achieved. After this runs full-strut has burned a little bit in the bottom part at the sharp edge and full-strut has tarnished because of the heat fluxes. Maximum value of the static pressure was nearby full-strut location. It's worth noting that in this test series maximum value of the static pressure was higher than in runs where imitator-strut was installed with the same amount of the injected hydrogen.

5 Conclusions

Experimental investigation of the elliptical combustion chamber model at the connected-pipe facility T-131 TsAGI in wide range of conditions at the model's entry and value of the ER coefficient was carried out.

Self-ignition of the hydrogen was achieved at all investigated conditions but at the conditions corresponding to free-stream Mach number $M=7.4$ and low values of the ER coefficient burning wasn't stabilized.

When hydrogen was injected through semi-struts, it was increasing of the static pressure

inside the model 2.5-3 times in comparison with regime without hydrogen supply and peak of the static pressure was located nearby full-strut.

Some investigation of the influence of the imitator-strut presence on the hydrogen burning inside the model was carried out. It could be stated that burning was obtained in both cases with and without imitator-strut. However presence of the imitator-strut increased maximum value of the static pressure in the model's duct and shifted its peak a little bit upstream.

When fuel is injected through semi-struts and full-strut, static pressure was increased 3-5 times in comparison with 'cold' regime and increasing of the static pressure wasn't almost propagated to 2D and 3D nozzle sections.

Regimes at which increasing of the static pressure propagates so high upstream that could influence on the static pressure in supersonic part of the aerodynamic nozzle were defined. Such regimes are very dangerous for propulsion because could lead to buzzing of the intake.

Acknowledgements

This work was performed within the 'High Speed Experimental Fly Vehicles - International' project fostering International Cooperation on Civil High-Speed Air Transport Research. HEXAFLY-INT, coordinated by ESA-ESTEC, is supported by the EU within the 7th Framework Programme Theme 7 Transport, Contract no.: ACP3-GA-2014-620327 with additional support of the Russian Ministry of Trade and Industry. Further info on HEXAFLY-INT can be found on http://www.esa.int/techresources/hexafly_int.

References

- [1] Steelant J. and Langener T. The LAPCAT-MR2 hypersonic cruiser concept. 29th Congress of the International Council of the Aeronautical Sciences (ICAS), St. Peterburg, September 7-12, 2014.
- [2] Langener T., Steelant J., Karl S. and Hannemann K. Design and Optimization of a Small Scale $M=8$ Scramjet Propulsion System. Space Propulsion 2012. Bordeaux: AAAF/ESA/CNES, 2012.
- [3] Langener T., Steelant J., Karl S. and Hannemann K. Layout and Design Verification of a Small Scale

Scramjet Combustion Chamber. ISABE 2013. Busan,
Korea: ISABE-2013-1655, 2013.

Contact Author Email Address

Mailto:talyzin@tsagi.ru

Copyright Statement

The authors confirm that they, and/or their company or organization, hold copyright on all of the original material included in this paper. The authors also confirm that they have obtained permission, from the copyright holder of any third party material included in this paper, to publish it as part of their paper. The authors confirm that they give permission, or have obtained permission from the copyright holder of this paper, for the publication and distribution of this paper as part of the ICAS proceedings or as individual off-prints from the proceedings.